Eur. Phys. J. C (2016) 76:192
DOI 10.1140/epjc/s10052-016-4054-4

THE EUROPEAN PHYSICAL JOURNAL C

CrossMark

Regular Article - Theoretical Physics

Implication of the observed $e^+e^- \to p\bar{p}\pi^0$ for studying the $p\bar{p} \to \psi(3770)\pi^0$ process

Hao Xu[1,2,a], **Ju-Jun Xie**[1,3,4,b], **Xiang Liu**[1,2,4,c]

[1] Research Center for Hadron and CSR Physics, Lanzhou University and Institute of Modern Physics of CAS, Lanzhou 730000, China
[2] School of Physical Science and Technology, Lanzhou University, Lanzhou 730000, China
[3] Institute of Modern Physics, Chinese Academy of Sciences, Lanzhou 730000, China
[4] State Key Laboratory of Theoretical Physics, Institute of Theoretical Physics, Chinese Academy of Sciences, Beijing 100190, China

Received: 2 February 2016 / Accepted: 30 March 2016 / Published online: 9 April 2016
© The Author(s) 2016. This article is published with open access at Springerlink.com

Abstract We study the charmonium $p\bar{p} \to \psi(3770)\pi^0$ reaction using the effective Lagrangian approach where the contributions from well-established N^* states are considered, and all parameters are fixed in the process of $e^+e^- \to p\bar{p}\pi^0$ at center of mass energy $\sqrt{s} = 3.773\,\text{GeV}$. The experimental data on the line shape of the mass distribution of the $e^+e^- \to p\bar{p}\pi^0$ can be well reproduced. Based on the study of $e^+e^- \to p\bar{p}\pi^0$, the total and differential cross sections of the $p\bar{p} \to \psi(3770)\pi^0$ reaction are predicted. At the same time we evaluated also the cross sections of the $p\bar{p} \to \psi(3686)\pi^0$ reaction. It is shown that the contribution of the nucleon pole to this reaction is largest close to the reaction threshold. However, the interference between nucleon pole and the other nucleon resonance can still change the angle distributions significantly. Those theoretical results may be tested by the future experiments at $\overline{\text{P}}$ANDA.

1 Introduction

As a forthcoming facility in the future, the Anti-Proton Annihilations at Darmstadt ($\overline{\text{P}}$ANDA) experiment will focus on the production of charmonium, which is governed by nonperturbative effects of quantum chromodynamics (QCD) [1]. Before the $\overline{\text{P}}$ANDA run, there were pioneering theoretical studies of the charmonium production in the $p\bar{p}$ annihilation processes [2–9]. By calculating two hadron-level diagrams introduced by the Born approximation, Gaillard and Maiani first studied the differential cross section of the charmonium production plus a soft pion in the $p\bar{p}$ reaction [2]. In Ref. [3], the cross sections of the charmonium (Ψ) production accompanied by a light meson (m) from the process of $p\bar{p} \to \Psi + m$ was calculated by combining with the measured partial decay widths of charmonium decay into $p\bar{p}m$. Then Barnes and Li proposed an initial state light meson emission model for the near threshold associated charmonium production processes $p\bar{p} \to \pi^0\Psi$ ($\Psi = \eta_c,\ J/\psi,\ \psi',\ \chi_{c0},\ \chi_{c1}$), and the total and differential cross sections for these reactions were evaluated [4–6]. It is also found that the cross section of $p\bar{p} \to \pi^0\Psi$ near threshold may be affected by the Pauli $J/\psi p\bar{p}$ coupling [5]. Furthermore, Lin, Xu and Liu revisited the issue of the production of charmonium plus a light meson at $\overline{\text{P}}$ANDA, where the contributions of the form factors (FFs) to these processes are included [7]. Recently, Pire et al. studied the associated production of a J/ψ and a pion in antiproton–nucleon annihilation in the framework of QCD collinear factorization [8], while in Ref. [9], the exclusive charmonium production process $p\bar{p} \to \pi^0 J/\psi$ was studied within a nucleon-pole exchange model by including off-shell hadronic FFs and a complete Lorentz structure with a $\bar{p}pJ/\psi$ Pauli strong coupling. The contributions from the intermediate N^* states are also studied in Ref. [9], and it was found that one cannot ignore the contributions of the N^* resonances in the $\bar{p}p \to \pi^0 J/\psi$ reaction.

The experimental activity on the charmonium decays have run in parallel. These decays are of interest because they can be used to study the associated charomonium production in $p\bar{p}$ annihilation. In 2014, the BESIII Collaboration reported the analysis of $e^+e^- \to p\bar{p}\pi^0$ in the vicinity of $\psi(3770)$ [10]. In addition to the Born cross section of $e^+e^- \to p\bar{p}\pi^0$, the corresponding $p\pi^0$ and $\bar{p}\pi^0$ invariant mass distributions of $e^+e^- \to p\bar{p}\pi^0$ process are also measured [10]. This new experimental information in Ref. [10] allows us to further perform a comprehensive study of $e^+e^- \to \psi(3770) \to p\bar{p}\pi^0$, which stimulates our interest to study the contribution of excited nucleon resonances

[a] e-mail: xuh2013@lzu.cn
[b] e-mail: xiejujun@impcas.ac.cn
[c] e-mail: xiangliu@lzu.edu.cn

(N^*) to $e^+e^- \to \psi(3770) \to p\bar{p}\pi^0$ and $\psi(3770)$ production from the $p\bar{p} \to \psi(3770)\pi^0$ reaction.

The nucleon is the simplest system in which the three colors of QCD can combine to form a colorless object, thus it is important to understand the internal quark–gluon structure of the nucleon and its excited N^* states, and the study of excited N^* states is an interesting research field of hadron physics [11], which can make our knowledge of hadron spectrum abundant. A very important source of information for the nucleon internal structure is the N^* mass spectrum as well as its various production and decay rates, while the charmonium decay into $p\bar{p}\pi^0$ is an ideal platform to study excited N^* nucleon resonances, because it provides an effective isospin 1/2 filter for the πN system due to isospin conservation [12–14].

In this work, we introduce excited N^* nucleon resonances in the process of $e^+e^- \to \psi(3770) \to p\bar{p}\pi^0$. By fitting the $p\pi^0$ and $\bar{p}\pi^0$ invariant mass distributions of the cross section of $e^+e^- \to p\bar{p}\pi^0$, we extract the information of couplings of $N^*N\pi$ and $\psi(3770)N^*\bar{N}$, which not only reflects the inner features of the discussed N^*, but also it helps us to learn the role played by N^* in the $e^+e^- \to \psi(3770) \to p\bar{p}\pi^0$.

Based on our study of the $e^+e^- \to \psi(3770) \to p\bar{p}\pi^0$ process, we move forward to study the $p\bar{p} \to \psi(3770)\pi^0$ reaction, which is due to the cross relation between the $\psi(3770) \to p\bar{p}\pi^0$ decay and the $p\bar{p} \to \psi(3770)\pi^0$ reaction [13]. Here, these extracted parameters from our study of $e^+e^- \to \psi(3770) \to p\bar{p}\pi^0$ will be employed to estimate the production rate of $p\bar{p} \to \psi(3770)\pi^0$ and relevant features. We calculate the total and differential cross sections of the $p\bar{p} \to \psi(3770)\pi^0$ reaction. It is shown that the contribution of the nucleon pole to this reaction is largest close to the reaction threshold. However, the interference between nucleon pole and the other nucleon resonance affects significantly and could change the angle distributions clearly. Additionally, there were abundant experimental data of $\psi(3686) \to p\bar{p}\pi^0$ given by BESIII [14], where BESIII released the branching ratio $B(\psi(3686) \to p\bar{p}\pi^0) = (1.65 \pm 0.03 \pm 0.15) \times 10^{-4}$ and the measured $p\pi^0$ and $\bar{p}\pi^0$ invariant mass spectra [14]. This experimental status related to $\psi(3686)$ lets us extend the above study to the $\psi(3686) \to p\bar{p}\pi^0$ decay, and also the $p\bar{p} \to \psi(3686)\pi^0$ reaction. Our studies provide valuable information to a future experimental exploration of $\psi(3770)$ and $\psi(3686)$ productions plus a pion through the $p\bar{p}$ interaction at $\overline{\mathrm{P}}$ANDA.

This paper is organized as follows. After the introduction in Sect. 1, we present a detailed study of $e^+e^- \to p\bar{p}\pi^0$ by including the excited N^* nucleon resonances (see Sect. 2). In Sect. 3, we further calculate $p\bar{p} \to \psi(3770)\pi^0$ by combining with these results obtained in Sect. 2. In Sect. 4, we adopt a similar approach to study $\psi(3686) \to p\bar{p}\pi^0$ decay and the $p\bar{p} \to \psi(3686)\pi^0$ process. The paper ends with a discussion and conclusion.

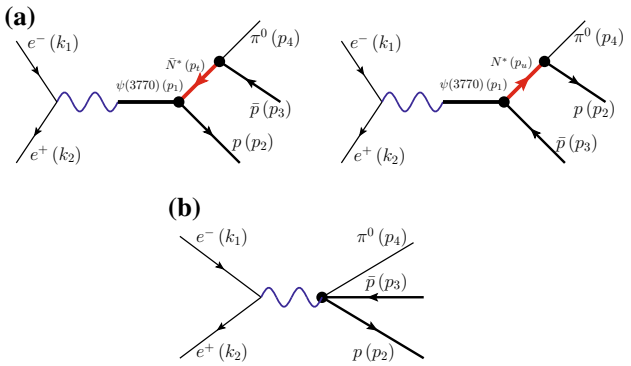

Fig. 1 (color online) The Feynman diagrams for the process $e^+e^- \to p\bar{p}\pi^0$ in the vicinity of $\psi(3770)$

2 Excited N^* nucleon resonance contributions to $e^+e^- \to \psi(3770) \to p\bar{p}\pi^0$

First, we study the process $e^+e^- \to p\bar{p}\pi^0$ with an effective Lagrangian approach. On the hadron level, the process $e^+e^- \to p\bar{p}\pi^0$ in the vicinity of $\psi(3770)$ is described by the diagrams shown in Fig. 1. In Fig. 1a, e^+ and e^- annihilate into a photon, which couples with charmonium $\psi(3770)$. Then $\psi(3770)$ interacts with the final states, where we consider the contributions from the nucleon pole ($\equiv P_{11}$) with $J^P = \frac{1}{2}^+$ and five N^* states that are well established [15]: $N(1440)$ ($\equiv P_{11}$) with $J^P = \frac{1}{2}^+$, $N(1520)$ ($\equiv D_{13}$) with $J^P = \frac{3}{2}^-$, $N(1535)$ ($\equiv S_{11}$) with $J^P = \frac{1}{2}^-$, $N(1650)$ ($\equiv S_{11}$) with $J^P = \frac{1}{2}^-$, and $N(1720)$ ($\equiv P_{13}$) with $J^P = \frac{3}{2}^+$. Additionally, we also consider the background contribution, where the e^+e^- annihilation is directly into $p\bar{p}\pi$ without intermediate $\psi(3770)$, which is shown in Fig. 1b.

To compute the contributions of these terms, we use the effective interaction Lagrangian densities for each vertex. For the $\gamma\psi(3770)$ coupling, we adopt the vector meson dominant (VMD) model, where a vector meson coupled to a photon is described by [16]

$$\mathcal{L}_{V\gamma} = -\frac{eM_V^2}{f_V} V_\mu A^\mu. \tag{1}$$

In the above expression, M_V and f_V are the mass and the decay constant of the vector meson, respectively. The decay constant e/f_V can be fitted through $V \to e^+e^-$:

$$e/f_V = \left[\frac{3\Gamma_{V\to e^+e^-}M_V^2}{8\alpha|\vec{p}|^3}\right]^{1/2} \simeq \left[\frac{3\Gamma_{V\to e^+e^-}}{\alpha M_V}\right]^{1/2}, \tag{2}$$

where $|\vec{p}| = (M_V^2 - 4m_e^2)^{1/2}/2 \simeq M_V/2$ is the three momentum of an electron in the rest frame of the vector meson. We have $\alpha = e^2/(4\pi) = 1/137$. Using $B(\psi(3770) \to e^+e^-) = (9.6 \pm 0.7) \times 10^{-6}$ [15], we obtain $e/f_{\psi(3770)} = 0.0053$.

The $J/\psi N\bar{N}$ and $NN\pi$ couplings are described by

$$\mathcal{L}_{\pi NN} = -\frac{g_{\pi NN}}{2m_N}\bar{N}\gamma_5\gamma_\mu\tau\cdot\partial^\mu\pi N, \tag{3}$$

$$\mathcal{L}_{\psi NN} = -g_{\psi NN}\bar{N}\gamma_\mu V^\mu N, \tag{4}$$

where V^μ stands for the vector field of $\psi(3770)$. We take $g_{\pi NN} = 13.45$.

For the $N^*N\pi$ and $\psi N^*\bar{N}$ vertices, we adopt the Lagrangian densities as used in Refs. [17–24]:

$$\mathcal{L}_{\pi NP_{11}} = -\frac{g_{\pi NP_{11}}}{2m_N}\bar{N}\gamma_5\gamma_\mu\tau\cdot\partial^\mu\pi R_{P_{11}} + h.c., \tag{5}$$

$$\mathcal{L}_{\pi NS_{11}} = -g_{\pi NS_{11}}\bar{N}\tau\cdot\pi R_{S_{11}} + h.c., \tag{6}$$

$$\mathcal{L}_{\pi NP_{13}} = -\frac{g_{\pi NP_{13}}}{m_N}\bar{N}\tau\cdot\partial_\mu\pi R^\mu_{P_{13}} + h.c., \tag{7}$$

$$\mathcal{L}_{\pi ND_{13}} = -\frac{g_{\pi ND_{13}}}{m_N^2}\bar{N}\gamma_5\gamma^\mu\tau\cdot\partial_\mu\partial_\nu\pi R^\nu_{D_{13}} + h.c., \tag{8}$$

$$\mathcal{L}_{\psi NP_{11}} = -g_{\psi NP_{11}}\bar{N}\gamma_\mu V^\mu R_{P_{11}} + h.c., \tag{9}$$

$$\mathcal{L}_{\psi NS_{11}} = -g_{\psi NS_{11}}\bar{N}\gamma_5\gamma_\mu V^\mu R_{S_{11}} + h.c., \tag{10}$$

$$\mathcal{L}_{\psi NP_{13}} = -ig_{\psi NP_{13}}\bar{N}\gamma_5 V_\mu R^\mu_{P_{13}} + h.c., \tag{11}$$

$$\mathcal{L}_{\psi ND_{13}} = -g_{\psi ND_{13}}\bar{N}V_\mu R^\mu_{D_{13}} + h.c., \tag{12}$$

where R is a N^* field.

For the intermediate nucleon-pole or N^* state, the Breit–Wigner form of the propagator $G_J(q)$ can be written as [25]

$$G_{\frac{1}{2}}(q) = i\frac{\not{q} + M_{N^*}}{q^2 - M^2_{N^*} + iM_{N^*}\Gamma_{N^*}} \tag{13}$$

for $J = \frac{1}{2}$, and

$$G^{\mu\nu}_{\frac{3}{2}}(q) = i\frac{\not{q} + M_{N^*}}{q^2 - M^2_{N^*} + iM_{N^*}\Gamma_{N^*}}\Big(-g_{\mu\nu} + \frac{1}{3}\gamma_\mu\gamma_\nu + \frac{1}{3m}(\gamma_\mu q_\nu - \gamma_\nu q_\mu) + \frac{2}{3}\frac{q_\mu q_\nu}{q^2}\Big) \tag{14}$$

for $J = \frac{3}{2}$. In Eqs. (13) and (14), M_{N^*} and Γ_{N^*} are the masses and widths of these intermediate N^* states, respectively. The values used in the present work for M_{N^*} and Γ_{N^*} are summarized in Table 1.

Table 1 Relevant resonant parameters for N^* states

N^*	M_{N^*} (MeV)	Γ_{N^*} (MeV)
$N(938)$	938	0
$N(1440)$	1430	350
$N(1520)$	1515	115
$N(1535)$	1535	150
$N(1650)$	1655	140
$N(1720)$	1720	250

The values are taken from the Particle Data Book [15]

On the other hand, we also need to introduce the form factors for these intermediate off-shell N^* (N), which are taken as in Refs. [26–29]:

$$F(q^2) = \frac{\Lambda^4}{\Lambda^4 + (q^2 - M^2_{N^*})^2}, \tag{15}$$

where the cut-off parameter Λ can be parameterized as

$$\Lambda = M_{N^*} + \beta\Lambda_{\rm QCD}, \tag{16}$$

with $\Lambda_{\rm QCD} = 220$ MeV. The parameter β will be determined by fitting the experimental data.

For the background contribution depicted in Fig. 1b, we construct the amplitude in analogy of Ref. [30]:

$$\mathcal{M}_{\rm NoR} = g_{\rm NoR}\bar{v}(k_2)e\gamma^\mu u(k_1)\frac{1}{s}\bar{u}(p_2)\gamma^\mu\gamma_5 v(p_3)\mathcal{F}_{\rm NoR}(s), \tag{17}$$

with $\mathcal{F}_{\rm NoR}(s) = \exp(-a(\sqrt{s} - \sum_f m_f)^2)$, where $\sum_f m_f$ means the mass of the final states are summed over. The parameter a will be fitted to the experimental measurements, and s is the invariant mass square of the e^+e^- system.

In the phenomenological Lagrangian approaches, the relative phases between amplitudes from different diagrams are not fixed. Generally, we should introduce a relative phase between different amplitudes as free parameters, and the total amplitude can be written as

$$\begin{aligned}\mathcal{M}_{e^+e^-\to p\bar{p}\pi^0} &= \mathcal{M}_{\rm NoR}e^{i\phi_{\rm NoR}} + \bar{v}(k_2)e\gamma^\mu u(k_1)\frac{-g^{\mu\nu}}{s}em^2_\psi/f_\psi \\ &\times\frac{-g_{\nu\alpha} + \frac{p_{\psi\nu}p_{\psi\alpha}}{m^2_\psi}}{s - m^2_\psi + im_\psi\Gamma_\psi}\left(\mathcal{M}^\alpha_N + \sum_{N^*}\mathcal{M}^\alpha_{N^*}e^{i\phi_{N^*}}\right),\end{aligned} \tag{18}$$

where $\mathcal{M}^\alpha_{N^*(N)}$, describing the subprocesses $\psi(3770) \to p\bar{p}\pi^0$, are given completely in the appendix.

The differential cross section is given by [31]

$$d\sigma_{e^+e^-\to p\bar{p}\pi^0} = \frac{(2\pi)^4\sum|\mathcal{M}_{e^+e^-\to p\bar{p}\pi^0}|^2}{4\sqrt{(k_1\cdot k_2)^2}}d\Phi_3, \tag{19}$$

and the phase space factor is given by

$$d\Phi_3 = \frac{1}{(2\pi)^9}\frac{1}{8\sqrt{s}}|\vec{p}^*_3||\vec{p}_2|d\Omega^*_3 d\Omega_2 dm_{\bar{p}\pi}, \tag{20}$$

with $\sum|\mathcal{M}|^2$ averaging over the spins of the initial e^+e^- and summing over the polarizations of the final states $p\bar{p}$.

As we can see in the appendix, in the tree-level approximation, only the products like $g_{N^*} \equiv g_{VNN^*}g_{\pi NN^*}$ enter in the invariant amplitudes. They are determined with the use of MINUIT, by fitting to the low energy experimental data on mass distribution of $e^+e^- \to p\bar{p}\pi^0$ at $\sqrt{s} = 3.773$ GeV [10]. So far we have 15 unknown parameters: six g_{N^*}, six phase angles, ϕ_{N^*} and $\phi_{\rm NoR}$, one cut-off, β,

Table 2 The fitted parameters in the process $e^+e^- \to p\bar{p}\pi^0$, where $g_{N^*} = g_{\psi(3770)NN^*}g_{\pi NN^*}$

N^*	g_{N^*} $(\times 10^{-3})$	ϕ_{N^*} (rad)
$N(938)$	8.00 ± 0.46	–
$N(1440)$	1.92 ± 0.98	6.09 ± 0.38
$N(1520)$	0.28 ± 0.24	3.74 ± 1.07
$N(1535)$	1.74 ± 1.34	2.99 ± 0.67
$N(1650)$	1.99 ± 0.18	2.17 ± 0.19
$N(1720)$	1.14 ± 0.63	6.02 ± 0.71

For nucleon, g_N is defined as $g_N = g_{\psi(3770)NN}g_{\pi NN}$

in the form factors and two parameters, $g_{\rm NoR}$ and a, in the direct production amplitude Eq. (17). We perform those 15-parameter χ^2 fits to the BESIII experiment data on the invariant mass distribution at 3.773 GeV below 1.8 GeV, and make use of the total cross-section information in Ref. [10]. Here, we do not consider the invariant mass region beyond 1.8 GeV, which contains a large contribution from higher mass N^* states and another complicated resonance which decays to $p\bar{p}$. In Ref. [9], it was pointed out that in the case of the $\bar{p}p \to \pi^0 J/\psi$ reaction the higher mass N^* resonances are needed. Indeed, in the present case, if we go beyond 1.8 GeV, we need also the higher mass N^* states. On the other hand, we did also another calculation including the contributions of higher spin nuclear excited states, $N(1675)5/2^-$ and $N(1680)5/2^+$. It is found that their contributions are quite small and the fitted parameters for the other nuclear resonance are little changed. Thus, we will not include the contributions of these two states in this work.

We get a minimal $\chi^2/dof = 1.03$ with the fitted cut-off parameter $\beta = 6.2 \pm 3.5$. The parameters appearing in the direct amplitude Eq. (17) are $g_{\rm NoR} = 0.45 \pm 0.02$, $\phi_{\rm NoR} = 4.84 \pm 0.20$ Rad and $a = 0.84 \pm 0.02$. The other fitted parameters are compiled in Table 2. The fitted results are shown in Fig. 2 compared with the experimental data taken from Ref. [10], where the green dashed line stands for the background contribution, the orange dotted line stands for the nucleon-pole contribution, the red line is the full result, and the other lines show the contributions from different N^* resonances. Notice that we have converted the experimental event to a physical differential cross section using the experimental value $\sigma_{\rm total} = 7.71$ pb at 3.773 GeV [10]. Our results can describe the two clear peaks around 1.5 and 1.7 GeV, thanks to the contributions from the $N(1520)$, $N(1535)$, and $N(1650)$ resonances. The contribution from the nucleon pole is small, while the background contribution is quite large.

In Fig. 2, it is interesting to see large interfering effects between different contributions. At the low $M_{\bar{p}\pi}$ region around 1.1–1.3 GeV, a large cancellation between the nucleon pole and the background leads to a quite suppressed spectrum, and the bump structure from the nucleon pole just disappears. From the two-peak region around 1.4–1.8 GeV, we can directly see that the background contribution plus N^* contribution (means without interfering contribution) is not able to reach the data peak, it indicates a large enhancement between the background contribution and the N^* contribution thanks to the interfering effect.

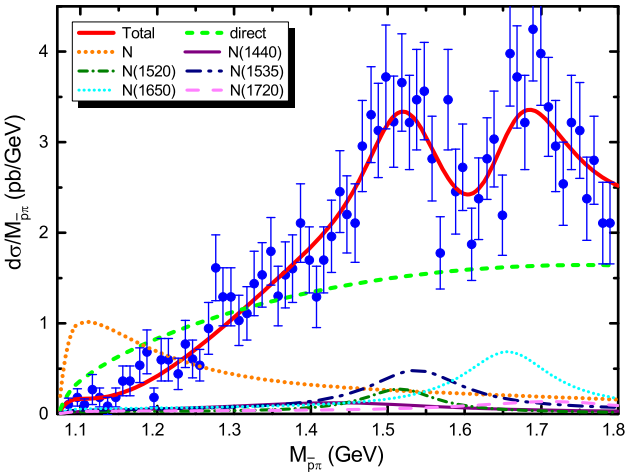

Fig. 2 (color online) The fitted mass spectrum of the process $e^+e^- \to p\bar{p}\pi^0$ at $\sqrt{s} = 3.773$ GeV comparing to the experiment data. The experiment data are taken from Ref. [10]. The *green dashed line* stands for the background contribution, the *orange dotted line* stands for the nucleon-pole contribution, the *red line* is the full result, and the *other lines* show the contributions from different N^* resonances. Notice that the experimental event is converted to a physical differential cross section using the experimental total cross section at $\sqrt{s} = 3.773$ GeV [10]

3 The $\psi(3770)$ production in the process $p\bar{p} \to \psi(3770)\pi^0$

A charmonium plus a light meson π can be produced by the low energy $p\bar{p}$ annihilation process. The tree-level diagrams for the $p\bar{p} \to \psi(3770)\pi^0$ reaction are depicted in Fig. 3. It is worth to mention that the effect of the N^* resonances in the cross channel of Fig. 3 has been studied first in the $\bar{p}p \to \pi^0 J/\psi$ reaction [9]. It was found that the contributions from the N^* resonances in the $\bar{p}p \to \pi^0 J/\psi$ reaction are important. In the present work, we extend the model

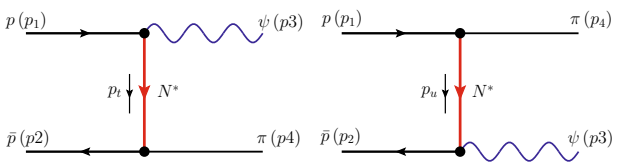

Fig. 3 (color online) The typical Feynman diagrams for the process $p\bar{p} \to \pi^0\psi(3770)$

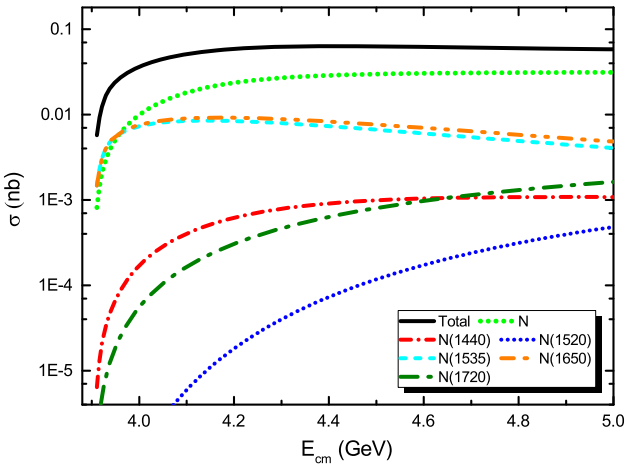

Fig. 4 (color online) Total cross section of the $p\bar{p} \to \pi^0\psi(3770)$ reaction. The *black line* is the total result, and the *other lines* show the contributions from different N^* resonances

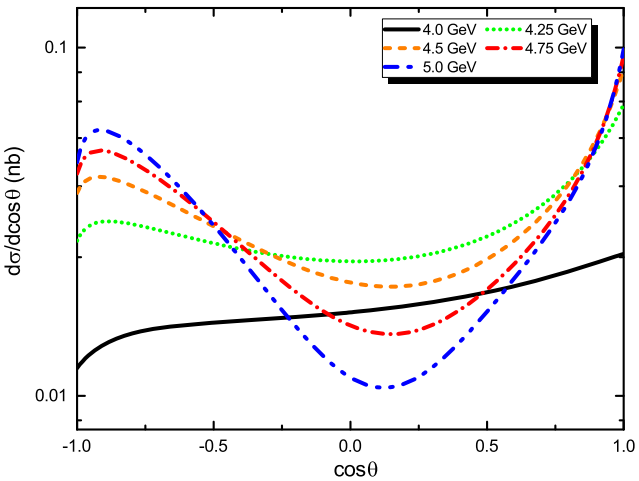

Fig. 5 (color online) Angular distributions of the $p\bar{p} \to \pi^0\psi(3770)$ reaction with full contribution

of Ref. [9] to the process of the higher charmonium states [$\psi(3770)$ and $\psi(3686)$] production.[1]

The differential cross section of the $p\bar{p} \to \pi^0\psi(3770)$ reaction in the center of mass (c.m.) frame can be expressed as [15]

$$\frac{d\sigma_{p\bar{p}\to\pi^0\psi(3770)}}{d\cos\theta} = \frac{1}{32\pi s}\frac{|\vec{p}_3^{\,\rm cm}|}{|\vec{p}_1^{\,\rm cm}|}\sum\overline{|\mathcal{M}|^2}, \tag{21}$$

where θ denotes the angle of the outgoing π^0 relative to beam direction in the c.m. frame, $\vec{p}_1^{\,\rm cm}$ and $\vec{p}_3^{\,\rm cm}$ are the three-momentum of the proton and $\psi(3770)$ in c.m. frame, respectively, while the total invariant scattering amplitude $\mathcal{M}$ is given in the appendix using the crossing symmetry.

With the parameters determined from the process of $e^+e^- \to p\bar{p}\pi^0$, we calculate the total and differential cross sections of the $p\bar{p} \to \pi^0\psi(3770)$ reaction. In Fig. 4, we show our results for the total cross section of the $p\bar{p} \to \pi^0\psi(3770)$ reaction as a function of the invariant mass ($E_{\rm cm}$) of $\bar{p}p$ system. At $E_{\rm cm} = 5.26$ GeV, the total cross section is 0.056 nb, and it is under the upper limit of the value obtained in Ref. [10].

From Fig. 4, we see that the nucleon pole gives the largest contribution, and it becomes dominant in the region $E_{\rm cm} > 5.0$ GeV. This is because in the reaction of $p\bar{p} \to \psi(3770)\pi^0$, the four-momentum square, q^2, of the nucleon or another nucleon resonance is smaller than 0, and the propagator $\frac{1}{q^2-M^2}$ will increase the contribution of the nucleon because of its small mass. Besides, it is found that the contributions from the N^* state with different quantum numbers have a quite different behavior. The contributions from $N(1535)$ and $N(1650)$ with $J^P = \frac{1}{2}^-$ decrease at $E_{\rm cm}$ around 4.2 GeV, while the others increase all the time. Overall, the total cross section becomes quite flat, while $E_{\rm cm} >$ 4.1 GeV.

In addition, we also calculate the angular distribution of the $p\bar{p} \to \pi^0\psi(3770)$ reaction at $E_{\rm cm} = 4.0, 4.25, 4.5, 4.75$ and 5.0 GeV. The numerical results are shown in Fig. 5. We can see that there emerges an obvious peak at the backward angles (around $\cos\theta \sim -0.8$) at $E_{\rm cm} \geq 4.25$ GeV produced by the contributions of the nucleon results in the u-channel, while the larger results at the forward angles are due to the t-channel nucleon resonances contributions.

In Fig. 6, we show the numerical results of the angular distributions by only considering the contribution from the nucleon pole. We can see that the angular distributions are symmetrical between the backward and forward angles.

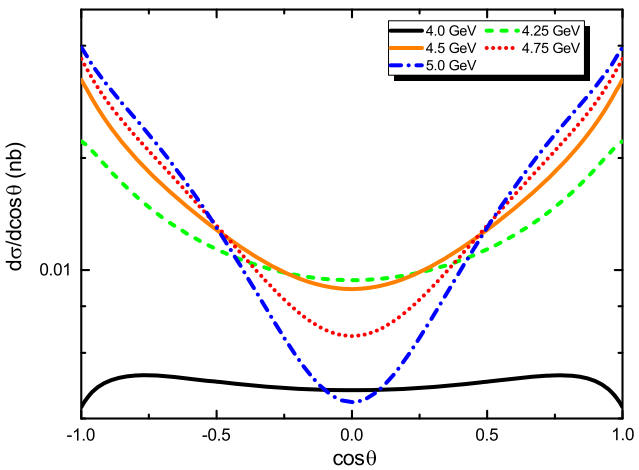

Fig. 6 (color online) Angular distributions of the $p\bar{p} \to \pi^0\psi(3770)$ reaction considered only the contribution from the nucleon pole

[1] We mention that the Regge exchange may be important; unfortunately, the information of the Regge propagators is scarce and we hope we can include the Regge contribution in the future.

Comparing Fig. 5 with Fig. 6, we see that there is a big difference between the full contribution and the nucleon-only contribution. Our model predictions may be tested by the future experiments.

Note that the exchanged nuclear resonances in Fig. 3 are far off mass shell, and the form factors for the exchanged nuclear resonances here should be different from those that have been used for the $e^-e^+ \to \psi(3770) \to p\bar{p}\pi^0$ reaction. We know that the form factors can be directly related to the hadron structure. However, the question of the hadron structure is still very open; we have to adjust the form factor to fit the experimental data, and the hadronic form factors are commonly used phenomenologically [26–29]. The effects of these form factors could substantially change the predicted cross sections. Because of the lack of the available experimental measurements, we cannot determine the form factors without ambiguities. In the present work, we take the same form factors for both the $\bar{p}p \to \psi(3770)\pi^0$ reaction and the $e^+e^- \to \psi(3770) \to \bar{p}p\pi^0$ reaction.

4 The implication for $\psi(3686) \to p\bar{p}\pi^0$ and $p\bar{p} \to \psi(3686)\pi^0$

For the process $\psi(3686) \to p\bar{p}\pi^0$, we first determine the coupling constant $g_{\psi(3686)NN}$, i.e., by using the Lagrangian in Eq. (4), $g_{\psi(3686)NN}$ can be fitted through the process $\psi(3686) \to p\bar{p}$. With the experimental value [15] $B(\psi(3686) \to p\bar{p}) = 2.8 \times 10^{-4}$, $g_{\psi(3686)NN}$ is determined to be

$$g_{\psi(3686)NN} = 9.4 \times 10^{-4}, \tag{22}$$

which is consistent with that given in Ref. [4].

In Ref. [14], BESIII released the $p\pi$ invariant mass spectrum of the process $\psi(3686) \to p\bar{p}\pi^0$ and decay width $\Gamma(\psi(3686) \to p\bar{p}\pi^0) = (1.65 \pm 0.03 \pm 0.15) \times 10^{-5}$. Similar to the case of $\psi(3770)$, we fit five coupling constants, g_{N^*}, five phase angles, and a cut-off parameter, β, to the experimental data. The fitted results are shown in Fig. 7. Here, one gets $\chi^2/d.o.f = 2.90$ and $\beta = 3.28 \pm 2.23$, while the fitted coupling constants g_{N^*} and the phase angles are listed in Table 3.

In Fig. 7, the dashed curve stands for the contribution of the nucleon pole, the solid line stands for the full contributions, and the other lines show the contributions from different N^* resonances. We see that we can describe the experimental data fairly well. Furthermore, we find that the peak between 1.6 and 1.7 GeV mainly comes from the contribution of $N(1650)$.

There also exist quite obvious interfering effects between different N^* contributions in Fig. 7. Close to $M_{p\pi} = 1.6$ GeV, comparing the $N(1440)$ contribution to the total

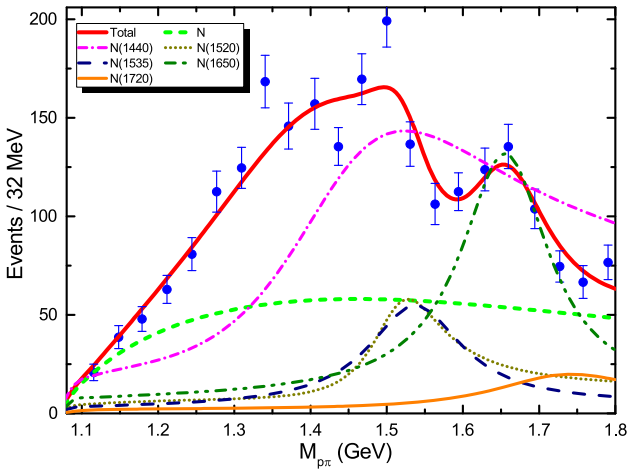

Fig. 7 (color online) The fitted $p\pi$ invariant mass spectrum of the process of $\psi(3686) \to p\bar{p}\pi^0$. The *dashed green curve* stands for the contribution of the nucleon pole, the *solid red line* stands for the full contributions, and the *other lines* show the contributions from different N^* resonances. The experiment data are taken from Ref. [14]

Table 3 Fitted coupling constants g_{N^*} and phase angles ϕ_{N^*} in the process $\psi(3686) \to p\bar{p}\pi^0$, where $g_{N^*} = g_{\psi(3686)NN^*}g_{\pi NN^*}$

N^*	g_{N^*} ($\times 10^{-3}$)	ϕ_{N^*} (rad)
$N(1440)$	5.10 ± 0.86	3.40 ± 0.22
$N(1520)$	2.27 ± 0.39	4.96 ± 1.10
$N(1535)$	0.51 ± 0.36	0.75 ± 0.64
$N(1650)$	0.76 ± 0.19	5.35 ± 0.92
$N(1720)$	0.98 ± 0.42	1.77 ± 0.99

contribution, one can see the $N(1440)$ contribution is "digged out" in a valley by other N^* contributions. In the region of $M_{p\pi} > 1.7$ GeV, the total contribution is smaller than the $N(1440)$ contribution, i.e., the total contribution is suppressed by interfering terms. So, from Figs. 2 and 7, one can see how important the interference effect is. We will not be able to get a good fit without interfering terms and arbitrary phase angles.

Additionally, we also calculated the branch fractions of $\psi(3686) \to (N^*\bar{p} + c.c.) \to p\bar{p}\pi^0$ from the individual intermediate N^* (or p) state, with the fitted coupling constants listed in Table 3. Our results are shown in Table 4. The errors of our theoretical results are obtained from the errors of those fitted coupling constants of g_{N^*}. We also notice that in Ref. [14] BESIII also extracted the corresponding branching fractions without considering the interference of different intermediate N^* (or p) states, which is different from the treatment in the present work. Thus, in Table 4 we further compare our result with the experimental results [14], and we see that our results are in agreement within errors with that given in Ref. [14].

Table 4 The calculated branching fractions $\psi(3686) \to p\bar{p}\pi^0$ if considering an individual intermediate N^* (or N) contribution, and the comparison with the experimental values of Ref. [14]

	Our results	The results in Ref. [14]
N	7.5	$6.42^{+0.20+1.78}_{-0.20-1.28}$
$N(1440)$	14 ± 4.5	$3.58^{+0.25+1.59}_{-0.25-0.84}$
$N(1520)$	2.8 ± 0.8	$0.64^{+0.05+0.22}_{-0.05-0.17}$
$N(1535)$	2.1 ± 3.0	$2.47^{+0.28+0.99}_{-0.28-0.97}$
$N(1650)$	4.9 ± 2.5	$3.76^{+0.28+1.37}_{-0.28-1.66}$
$N(1720)$	1.3 ± 1.0	$1.79^{+0.10+0.24}_{-0.10-0.71}$

Here, all values are in units of 10^{-5}

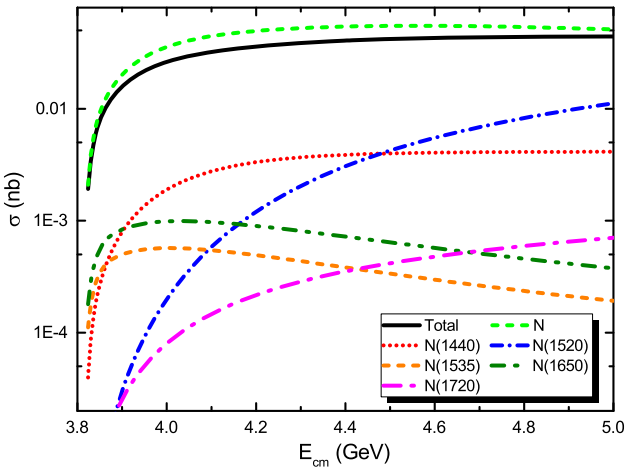

Fig. 8 (color online) The cross section of the process $p\bar{p} \to \pi^0\psi(3686)$. The *black line* is total result, and the *other lines* show the N^* contribution

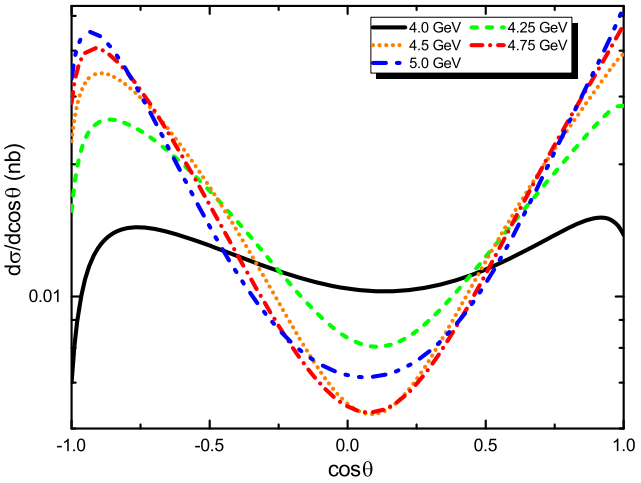

Fig. 9 (color online) The angular distribution of the process $p\bar{p} \to \pi^0\psi(3686)$. *Each line* shows a different c.m. energy

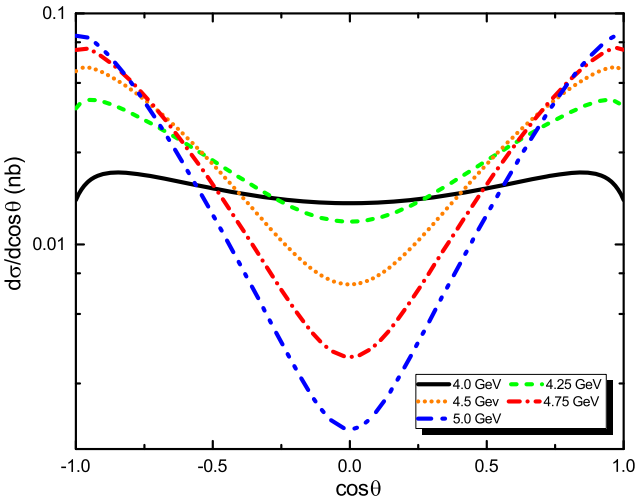

Fig. 10 (color online) The angular distribution of the process $p\bar{p} \to \pi^0\psi(3686)$ only considering the nucleon contribution. Each *line* shows a different c.m. energy

With these fitted parameters, we calculate the cross section of the process $p\bar{p} \to \pi^0\psi(3686)$ with crossing symmetry. The results are shown in Fig. 8. One can see that the nucleon-pole contribution is predominant in the whole energy region, while the contributions from the other N^* states are small. In the higher energy region, the nucleon-pole contribution starts to decrease, while the full contribution increases slowly, and this behavior resembles the process $p\bar{p} \to \pi^0\psi(3770)$. Furthermore, it is noticed that the discrepancy between the total result and the nucleon contribution is smaller than in the case of $p\bar{p} \to \pi^0\psi(3770)$.

Finally, we show the angular distributions of the process $p\bar{p} \to \pi^0\psi(3686)$ in Figs. 9 and 10. Similar to Fig. 5, there is a peak in the backward angle and a valley close to $\cos\theta = 0$. Comparing to the angular distribution with the nucleon contribution in Fig. 10, there exists an obvious difference, since the nucleon contribution only has symmetry, while the total contribution has asymmetry.

5 Discussion and conclusion

We have studied the $e^+e^- \to p\bar{p}\pi^0$ at 3.773 GeV c.m. energy and $p\bar{p} \to \pi^0\psi(3770)$ reaction within an effective Lagrangian approach. The $e^+e^- \to p\bar{p}\pi^0$ process is a good platform to study the excited N^* nucleon resonances. We consider contributions from the nucleon pole and five well-established N^* states. First, we perform a χ^2-fit to the experimental data on the mass distribution of the $e^+e^- \to p\bar{p}\pi^0$, from which we obtain the couplings of $\psi(3770)$ to these N^* states. It is shown that we can describe the experimental data quite well. In particular, the two bumps around 1.5 and 1.7 GeV can be well reproduced. We also find that the contribution of the nucleon pole is small compared to the

background contribution, and there exists a large cancellation in the low $M_{\bar{p}\pi}$ region.

Second, based on our results of the $e^+e^- \to p\bar{p}\pi^0$, we study the $p\bar{p} \to \pi^0\psi(3770)$ reaction with crossing symmetry. We evaluate the total and differential cross sections of the $p\bar{p} \to \pi^0\psi(3770)$ reaction. The nucleon pole gives the largest contribution to the $p\bar{p} \to \pi^0\psi(3770)$ reaction close to threshold. However, the interference terms between the nucleon pole and the other nucleon resonance affects significantly and could change the angle distributions clearly. Our studies provide valuable information for future experimental exploration of the $\psi(3770)\pi^0$ production through the $p\bar{p}$ interaction.

Additionally, we also study the $\psi(3686)$ production through the process $p\bar{p} \to \pi^0\psi(3686)$. Similarly to the case of $e^+e^- \to \psi(3770) \to p\bar{p}\pi^0$, we study first of all the decay process of $\psi(3686) \to p\bar{p}\pi^0$ to extract the parameters we needed. Then we study the $p\bar{p} \to \pi^0\psi(3686)$ reaction. We find that the contribution from the nucleon pole is dominant, while the angular distributions show quite a discrepancy induced by the N^* states.

We hope and expect that future experiments at $\overline{\text{P}}$ANDA will provide a test to our model and give more constraints on our theoretical study.

Acknowledgments This project is supported by the National Natural Science Foundation of China under Grants Nos. 11222547, 11175073, and 11475227, the Ministry of Education of China (SRFDP under Grant No. 2012021111000), and the Fok Ying Tung Education Foundation (Grant No. 131006). This work is also supported by the Open Project Program of State Key Laboratory of Theoretical Physics, Institute of Theoretical Physics, Chinese Academy of Sciences, China (No.Y5KF151CJ1).

Open Access This article is distributed under the terms of the Creative Commons Attribution 4.0 International License (http://creativecommons.org/licenses/by/4.0/), which permits unrestricted use, distribution, and reproduction in any medium, provided you give appropriate credit to the original author(s) and the source, provide a link to the Creative Commons license, and indicate if changes were made.
Funded by SCOAP[3].

Appendix: scattering amplitudes of the subprocess $\psi(3770) \to p\bar{p}\pi^0$ and the process $p\bar{p} \to \pi^0\psi(3770)$

The tree-level diagrams of the subprocess $\psi(3770) \to p\bar{p}\pi^0$ are depicted in part of Fig. 1a. According to the Feynman diagrams shown in Fig. 1, the scattering amplitudes $\mathcal{M}_{J^P}$ with an exchanged $N^*(J^P)$ (including N) are given by

$$\mathcal{M}_{\frac{1}{2}^+} = \frac{g_{\pi NP_{11}}}{2m_N} g_{VNP_{11}} \epsilon^\mu(p_1)\bar{u}(p_2) \times \left[\gamma_\mu \frac{-\not{p}_t + m_{N^*}}{t - m_{N^*}^2}\gamma_5(i\not{p}_4)F(t) + \gamma_5(i\not{p}_4) \times \frac{\not{p}_u + m_{N^*}}{u - m_{N^*}^2}\gamma_\mu F(u)\right] v(p_3), \quad (23)$$

$$\mathcal{M}_{\frac{1}{2}^-} = g_{\pi NS_{11}} g_{VNS_{11}} \epsilon^\mu(p_1)\bar{u}(p_2) \left[\gamma_5\gamma_\mu \frac{-\not{p}_t + m_{N^*}}{t - m_{N^*}^2}F(t) + \frac{\not{p}_u + m_{N^*}}{u - m_{N^*}^2}\gamma_5\gamma_\mu F(u)\right] v(p_3), \quad (24)$$

$$\mathcal{M}_{\frac{3}{2}^+} = \frac{g_{\pi NP_{13}}}{m_N} i g_{VNP_{13}} \epsilon^\mu(p_1)\bar{u}(p_2) \left[\gamma_5 \frac{-\not{p}_t + m_{N^*}}{t - m_{N^*}^2} G_{\mu\nu}(-p_t)(ip_4^\nu)F(t) + (ip_4^\nu)\frac{\not{p}_u + m_{N^*}}{u - m_{N^*}^2} G_{\nu\mu}(p_u)\gamma_5 F(u)\right] v(p_3), \quad (25)$$

$$\mathcal{M}_{\frac{3}{2}^-} = \frac{g_{\pi ND_{13}}}{m_N^2} g_{VND_{13}} \epsilon^\mu(p_1)\bar{u}(p_2) \left[\frac{-\not{p}_t + m_{N^*}}{t - m_{N^*}^2} G_{\mu\nu}(-p_t)\gamma_5(i\not{p}_4)(ip_4^\nu)F(t) + \gamma_5(i\not{p}_4)(ip_4^\nu)\frac{\not{p}_u + m_{N^*}}{u - m_{N^*}^2} G_{\nu\mu}(p_u)F(u)\right] v(p_3), \quad (26)$$

with $t = p_t^2 = (p_1 - p_2)^2$ and $u = p_u^2 = (p_1 - p_3)^2$, and $G_{\mu\nu}$ is

$$G_{\mu\nu}(p) = \left(-g_{\mu\nu} + \frac{1}{3}\gamma_\mu\gamma_\nu + \frac{1}{3m_{N^*}}(\gamma_\mu p_\nu - \gamma_\nu p_\mu) + \frac{2}{3}\frac{p_\mu p_\nu}{m_{N^*}^2}\right). \quad (27)$$

For $\mathcal{M}^\alpha_{N^*(N)}$ in Eq. (18), just drop the polarization vector $\epsilon^\mu(p_1)$.

For the $p\bar{p} \to \pi^0\psi(3770)$ reaction, the scattering amplitudes can easily be obtained just applying the substitution to Eqs. (23)–(26):

$$p_1 \to -p_3, \quad p_2 \to -p_2, \quad p_3 \to -p_1, \quad p_t \to -p_u. \quad (28)$$

The amplitudes of the processes $\psi(3686) \to p\bar{p}\pi^0$ and $p\bar{p} \to \pi^0\psi(3686)$ are exactly the same.

References

1. M.F.M. Lutz et al. [PANDA Collaboration], arXiv:0903.3905 [hep-ex]
2. M.K. Gaillard, L. Maiani, R. Petronzio, Phys. Lett. B **110**, 489 (1982)
3. A. Lundborg, T. Barnes, U. Wiedner, Phys. Rev. D **73**, 096003 (2006)
4. T. Barnes, X. Li, Phys. Rev. D **75**, 054018 (2007)
5. T. Barnes, X. Li, W. Roberts, Phys. Rev. D **77**, 056001 (2008)

6. T. Barnes, X. Li, W. Roberts, Phys. Rev. D **81**, 034025 (2010)
7. Q.Y. Lin, H.S. Xu, X. Liu, Phys. Rev. D **86**, 034007 (2012)
8. B. Pire, K. Semenov-Tian-Shansky, L. Szymanowski, Phys. Lett. B **724**, 99 (2013)
9. J. Van de Wiele, S. Ong, Eur. Phys. J. C **73**, 2640 (2013)
10. M. Ablikim et al. [BESIII Collaboration], Phys. Rev. D **90**, 032007 (2014)
11. E. Klempt, J.M. Richard, Rev. Mod. Phys. **82**, 1095 (2010)
12. M. Ablikim et al. [BES Collaboration], Phys. Rev. Lett. **97**, 062001 (2006)
13. T. Barnes, Int. J. Mod. Phys. Conf. Ser. **02**, 193 (2011)
14. M. Ablikim et al. [BESIII Collaboration], Phys. Rev. Lett. **110**, 022001 (2013)
15. K.A. Olive et al. [Particle Data Group Collaboration], Chin. Phys. C **38**, 090001 (2014)
16. Q.Y. Lin, X. Liu, H.S. Xu, Phys. Rev. D **88**, 114009 (2013)
17. K. Tsushima, A. Sibirtsev, A.W. Thomas, Phys. Lett. B **390**, 29 (1997)
18. K. Tsushima, A. Sibirtsev, A.W. Thomas, G.Q. Li, Phys. Rev. C **59**, 369(1999)
19. K. Tsushima, A. Sibirtsev, A.W. Thomas, G.Q. Li, Phys. Rev. C **61**, 029903 (2000)
20. B.S. Zou, F. Hussain, Phys. Rev. C **67**, 015204 (2003)
21. Z. Ouyang, J.J. Xie, B.S. Zou, H.S. Xu, Int. J. Mod. Phys. E **18**, 281 (2009)
22. J.J. Wu, Z. Ouyang, B.S. Zou, Phys. Rev. C **80**, 045211 (2009)
23. X. Cao, B.S. Zou, H.S. Xu, Phys. Rev. C **81**, 065201 (2010)
24. X. Cao, B.S. Zou, H.S. Xu, Nucl. Phys. A **861**, 23 (2011)
25. S.Z. Huang, P.F. Zhang, T.N. Ruan, Y.C. Zhu, Z.P. Zheng, Eur. Phys. J. C **42**, 375 (2005)
26. T. Feuster, U. Mosel, Phys. Rev. C **58**, 457 (1998)
27. H. Haberzettl, C. Bennhold, T. Mart, T. Feuster, Phys. Rev. C **58**, 40 (1998)
28. T. Yoshimoto, T. Sato, M. Arima, T.S.H. Lee, Phys. Rev. C **61**, 065203 (2000)
29. Y.S. Oh, A.I. Titov, T.S.H. Lee, Phys. Rev. C **63**, 025201 (2001)
30. D.Y. Chen, J. He, X. Liu, Phys. Rev. D **83**, 054021 (2011). arXiv:1012.5362 [hep-ph]
31. J.J. Xie, Y.B. Dong, X. Cao, Phys. Rev. D **92**, 034029 (2015)